

## Crystalline-to-amorphous transition for Si-ion irradiation of Si(100)

Peter J. Schultz,\* C. Jagadish, M. C. Ridgway, R. G. Elliman,<sup>†</sup> and J. S. Williams<sup>†</sup>

*Department of Electronic Materials Engineering, The Australian National University, G.P.O. Box 4, Canberra, Australia*

(Received 28 June 1991)

Silicon (100) crystals are implanted with 1-MeV  $\text{Si}^{2+}$  ions to a fixed fluence of  $1 \times 10^{15}$  ions/cm<sup>2</sup> at systematically different incident-ion dose rates,  $R$ , and substrate temperatures,  $T$ . A critical dependence on  $T$  is found for  $R_c$ , the critical flux for formation of a continuous amorphous layer in the substrate material. The activation energy characterizing the process is found to be  $0.9 \pm 0.05$  eV, which is attributed to the collapse of defect complexes formed during irradiation. Critical temperatures for this process, at each fixed dose rate, are all near room temperature.

The amorphization of silicon caused by irradiation with energetic ions has been studied for many years, but it is sufficiently complicated that the details of the process are still not clear. It has always been recognized that there is a critical fluence for amorphization  $\phi_c$  which is a function of both incident-ion species and energy.<sup>1,2</sup> In addition, it was noted early on that dynamic annealing *during* implantation is important, and thus both the temperature of the substrate *and* the ion flux, or dose rate ( $R$ ) during implantation are significant.<sup>3</sup> In spite of this early recognition, there has been very little done to explore this in detail until very recently. By irradiating silicon with rare-gas ions (Ne through Xe) it has been observed that for a given fluence and temperature there is a critical flux for amorphization, known as the amorphous threshold flux,  $R_c$ , which obeys an Arrhenius dependence on temperature with an activation energy of  $E_a = 1.2$  eV.<sup>4,5</sup> This value was found for the amorphization of a subsurface layer and for the balance between recrystallization and amorphization at a preexisting planar crystalline-amorphous interface, both processes occurring in the 400–550 K temperature regime for the ion fluxes employed. At these temperatures the divacancy [which has an activation energy for annealing of 1.2–1.3 eV (Refs. 6 and 7)] has a relatively short lifetime (on the order of seconds),<sup>3</sup> comparable to the time required for cascade overlap at these fluxes. The additional evidence that the ion dependence of the process obeys a bimolecular scaling<sup>5</sup> (i.e., defect density squared) combined with the similarity of the activation energies led to the conclusion that the stability of the silicon divacancy controls the observed crystalline-amorphous phase transition, at least in the 400–550 K temperature range studied. The dependence of this transition on divacancy annealing was first suggested by Vook and Stein.<sup>3</sup>

In this paper we present a systematic study of the temperature and flux dependence of the crystalline-amorphous transition for a fixed fluence of  $1 \times 10^{15}$  cm<sup>-2</sup>, 1-MeV  $\text{Si}^{2+}$  ions incident on (100) silicon substrates. The critical temperatures observed in the present study are all near room temperature (some below, some above). This is significant since the ion mass, energy, fluence, and flux are *all* in fairly typical ranges for a variety of implantation and damage studies reported in the literature recently, suggesting that beam heating effects could lead to variable results under nominally “identical” conditions unless spe-

cial care is taken to thermally couple the target wafer to a temperature-controlled holder. The data also support a similar thermally activated process of the model suggested by Vook and Stein.<sup>3</sup> However, under the near-room-temperature conditions of the present study the divacancy is extremely stable ( $\approx 10^5$  sec), and we find a lower activation energy of  $E_a = 0.9 \pm 0.05$  eV. This result is discussed in terms of both the stability and variety of defect complexes formed, which depend primarily on the substrate temperature during irradiation.

Czochralski grown (100) Si wafers (phosphorous doped, 2–4  $\Omega$  cm) were irradiated with  $\text{Si}^{2+}$  ions at 1 MeV using the 1.7 MV NEC Tandem implanter at the Australian National University (ANU). Dose rates from  $R = 2.63 \times 10^{13}$  to  $2.88 \times 10^{11}$  ions/cm<sup>2</sup>s (corresponding to beam currents of  $\sim 10$   $\mu$ A/cm<sup>2</sup> to  $\sim 10$  nA/cm<sup>2</sup>) resulted in irradiation times from several seconds to about 1 h per point. The incident beam was wobbling over a small (4 mm diam) aperture to ensure uniformity, and the intensity was held constant to within a few percent throughout each series of temperatures at a given flux. Samples were clamped to a large copper mounting block using high-vacuum grease to ensure good thermal contact. The temperature was maintained within  $\pm 1$  K during each implant, with an estimated relative precision of better than  $\pm 2$  K, and absolute accuracy of roughly  $\pm 5$  K.

Crystal damage was evaluated by analysis of the Rutherford-backscattering-channeling (RBSC) distributions measured with a surface-barrier detector at a scattering angle of 170°. For this analysis, a 20-nA incident beam of 2-MeV  $\text{He}^{2+}$  was produced by the 1 MV General Ionex Tandem accelerator at the Royal Melbourne Institute of Technology. A set of typical spectra for the lowest dose rate are shown in Fig. 1, clearly indicating the buildup of subsurface damage with decreasing substrate temperature by the increased RBSC signal near channel 140 (corresponding to a depth of  $\sim 1.3$   $\mu$ m). Two reference spectra are also shown for a random direction and for a perfectly aligned virgin Si(100) sample. No significant change is observed for implantation between temperatures of 320 K and  $\approx 400$  K, or even higher, indicating the data shown for 320 and 330 K reflect the minimum damage level for this fluence. It can be seen from Fig. 1 that the complete range of final states from the damaged to the fully amorphized layer occurs with a

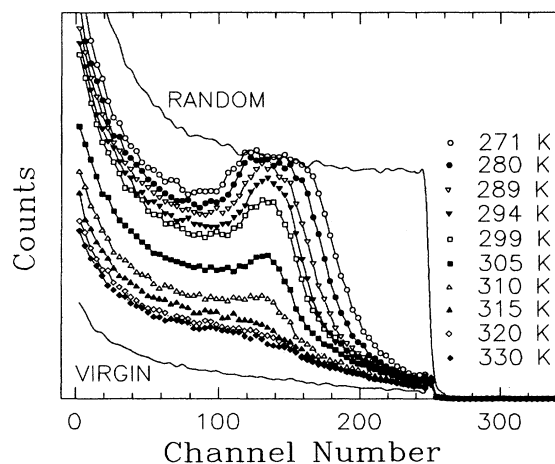


FIG. 1. Rutherford backscattering spectra for 2-MeV  $\text{He}^+$  channeled along the (100) direction of silicon samples. All data are for samples implanted with 1-MeV  $\text{Si}^+$  ions at the substrate temperatures indicated using a fixed flux of  $2.88 \times 10^{11}$  ions/cm<sup>2</sup>s, and a fixed fluence of  $1 \times 10^{15}$  ions/cm<sup>2</sup>, except the curve for the "virgin" material. The transition from minimally defected material ( $\geq 320$  K) to a continuous, buried amorphous layer ( $\leq 290$  K) is evident near channel No. 140.

change of just 25 K in substrate temperature, centered very near room temperature, where most implants reported in the literature are done. This variation is well within the limits of typical beam heating effects for MeV- $\mu\text{A}$  ion beams,<sup>8</sup> and demonstrates the need for adequate care in sample mounting<sup>9</sup> and the need to report the flux used for any given experiment.

Similar data to those shown in Fig. 1 were obtained for all dose rates. The extent of amorphization in the high damage end-of-range layer was parametrized by measuring the relative height of each curve between the virgin and amorphous samples. These damage yields  $Y_a$  are shown in Fig. 2 versus the substrate temperature during irradiation  $T$  and it can be seen that a similar characteristic shape is obtained for the transition from crystalline-amorphous for all dose rates, which we parametrize with a simple inverse exponential,

$$Y_a = a + b \left( \frac{1}{1 + \exp[\delta(T - T_c)]} \right). \quad (1)$$

The best fit of Eq. (1) to the data are the solid curves in Fig. 2. The constant  $\delta$  describes the width of the phase transition, and it is consistent for all dose rates ( $\delta = 0.19 \pm 0.02 \text{ K}^{-1}$ ). The critical temperature  $T_c$  at which the transition occurs is plotted in Fig. 3. The data show a simple exponential activation to within the limits of experimental accuracy, as would be expected for the kinetic model of damage nucleation proposed by Vook and Stein.<sup>3</sup> The best fit to the data in Fig. 3 yields an activation energy of  $E_a = 0.9 \pm 0.05 \text{ eV}$ , which is shown together with slopes of 0.8 and 1.0 eV.

Models for ion-beam induced amorphization vary from heterogeneous models in which amorphous zones are generated directly by the incident ions, to homogeneous models in which the average defect density is increased to a

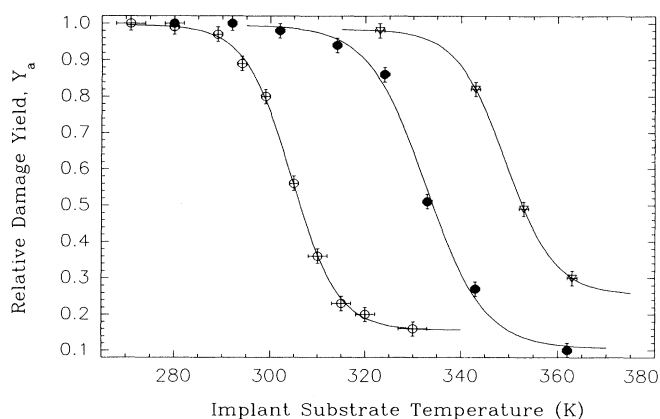


FIG. 2. The relative damage measured at channel 140 between the virgin (0.0) and random (1.0) curves. The data shown are for ion flux of the following:  $\circ$ :  $2.88 \times 10^{11}$  ions/cm<sup>2</sup>s;  $\bullet$ :  $3.57 \times 10^{12}$  ions/cm<sup>2</sup>s; and  $\nabla$ :  $2.63 \times 10^{13}$  ions/cm<sup>2</sup>s. The solid curves are the fit of Eq. (1) to the data, which yield the critical temperatures  $T_c$  that are plotted in Fig. 3.

level where the damaged crystal is unstable with respect to the amorphous phase. In the heterogeneous model, amorphous zones accumulate with increasing ion fluence, eventually overlapping to form a continuous amorphous layer. In the homogeneous model, defects accumulate with increasing fluence until the damaged crystal becomes metastable, and amorphous Si then nucleates and grows at the expense of the crystalline phase.

An ion flux dependence is expected for both heterogeneous and homogeneous amorphization processes. In both cases the instantaneous defect concentration and the resulting damage are expected to be functions of temperature and ion flux. In the heterogeneous case, amorphous zones will shrink if the temperature is sufficiently high. If the ion flux is low enough that the zones anneal prior to

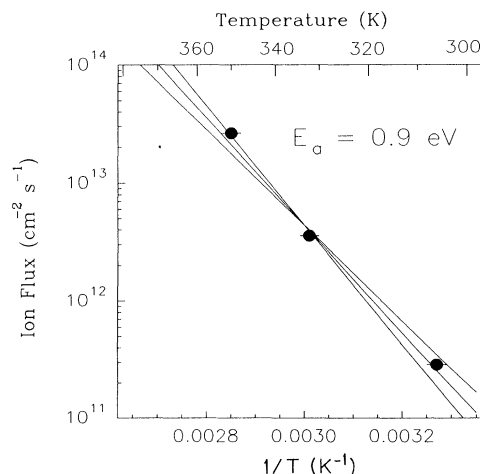


FIG. 3. Critical flux vs temperature for crystalline to amorphous transition, defined as illustrated in Fig. 2. The best fit to the Arrhenius distribution yields  $E_a = 0.9 \text{ eV}$ , which is shown together with slopes of 0.8 and 1.0 eV.

overlap, amorphization may never be achieved (except in the homogeneous limit where there is sufficient buildup of the residual damage). If the ion flux is sufficiently high to allow zone overlap before zone annihilation, then damage will accumulate. In the homogeneous case, the dynamical defect concentration during irradiation will also depend on a balance between defect creation and annihilation rates. If the ion flux is too low then defects will annihilate faster than they are created and the defect density may never exceed the critical value for amorphization.

In the limit of very low temperature, the amorphization process will eventually become athermal (i.e.,  $E_a \rightarrow 0$ ). At this point the balance between heterogeneous and homogeneous damage is determined solely by the energy deposition density, which depends only on the ion mass and energy, and defects that are formed are not greatly influenced by annealing processes. As a consequence, one might expect the measured activation energy to decrease as the temperature decreases, due to an increasing athermal component. At finite temperature, however, both heterogeneous and homogeneous damage nucleation processes could involve many different defects and their various annealing routes. In specific temperature regimes the temperature-ion flux dependence may be dominated by particularly stable defect configurations, and it is instructive to consider a more detailed view of defect production and interactions.

During implantation, each incident ion produces a damage volume around the track known as a damage cascade. In the absence of defect mobility, collisional processes dictate that vacancy-type defects are concentrated near the center of the cascade, while the outer perimeter is richer in interstitials. In silicon, self-interstitials are highly mobile and immediately recombine with vacancies, substitutional dopant impurities (Watkins replacement mechanism<sup>10</sup>), and/or combine to form more stable complexes (such as dislocation loops). Vacancies become mobile around 100 K, and can be trapped by oxygen impurities (known as the *A* center, common in Czochralski-grown Si), by the dopant atoms (*E* center, common in float zone Si), or combine to form divacancies. The impurity-bound centers are not expected to be critically involved in the crystalline-amorphous phase transition. As discussed above, the instability of the Si divacancy has been associated with the crystalline-amorphous transition at elevated temperatures. For the present data at  $\approx 300$  K, the divacancy is very stable and is clearly not responsible for limiting the structural phase transition. In this case it is reasonable to assume that the measured activation is in fact an average value for various, more complex defect structures. Extended multivacancy- or vacancy-impurity defect complexes can be formed either dynamically during irradiation or in post-irradiation thermal annealing of damaged material.<sup>11</sup>

Silicon is covalently bonded and fourfold coordinated. Amorphous silicon is made up of distorted five- and seven-member rings mixed with the six-member rings of the perfect crystal. Atomistic models for the crystalline-amorphous transition are based on the formation of complex multivacancy defects which ultimately result in the distorted ring structures, and the buildup of these defects

through the overlap of damage cascades.<sup>12</sup> Such models encompass elements of both heterogeneous and homogeneous damage nucleation processes, in allowing for initial high densities of complex damage within individual cascades, as well as the uniform buildup of a distributed damage base.

A particularly successful model of this type is based on the numerical simulations of Tan,<sup>13</sup> who modeled the nucleation of extended defects by assuming that the dominant factor in the configurational energy of the defects is the number of dangling bonds per point defect incorporated. He observes that the first stage is the condensation of point defects (both intrinsic, vacancies, and extrinsic, interstitials) along  $\langle 110 \rangle$  row configurations, which he calls intermediate defect configurations (IDCs). The vacancy IDC is just an arbitrary extension of a planar multivacancy, the simplest of which is the divacancy,<sup>14</sup> and the ultimate relaxation of the IDC (with no dangling bonds) is to adjacent pairs of five- and seven-membered rings, which is amorphous material. Such a model would exhibit a considerable dependence on temperature (and thus flux), since nucleation of the complex defect structures would in part be limited by point defect mobility. In the vicinity of each damage cascade, the Frenkel pairs would all be fully relaxed into divacancies and, to some extent IDCs, as well as stable dislocation loops. The planar tetravacancy, which is probably the most common vacancy-type defect formed at room temperature next to the divacancy, presumably has an even lower activation energy than the divacancy (it anneals at  $\sim 450$  K as opposed to  $\sim 570$  K for the divacancy),<sup>2</sup> and may be contributing to the "reduced" activation energy for the average defect distribution which controls the phase transition.

Returning to the rate equation description introduced by Vook and Stein,<sup>3</sup> where the accumulation of damage is balanced by dynamical annealing, it is possible to at least phenomenologically consolidate the atomistic IDC model with the simpler picture of a single, predominant defect process that is implied by the Arrhenius dependence of  $R_f$  on temperature, at least over the limited range of temperatures applicable to the present study. In this picture, each incident Si ion would create "stable" heterogeneous damage complexes and possibly small, localized, amorphous zones at the end of each cascade. These small heterogeneously formed disordered zones are the result of relaxation of highly mobile point defects created within the cascade through a mechanism such as the energy minimization which resulted in Tan's model for the IDC. The zones would dynamically shrink via point defect emission (either vacancies or self-interstitials), and the balance between the production rate of the zones (ion flux) and the rate of zone collapse would determine the critical temperature. This would suggest that the measured activation energy of 0.9 eV is associated in part with defect release from the disordered (possibly amorphous) zones, but in any case is an average of all competing processes.

In conclusion, we have measured the critical dependence on temperature and flux of the crystalline to amorphous transition in Si-ion irradiated Si(100). For a fixed fluence of 1 MeV,  $1 \times 10^{15}$  ions/cm<sup>2</sup>, it is shown that a complete transition from minimally defected to fully

amorphized material occurs within about  $\pm 10$  K on either side of the critical temperature, which in this case is very near room temperature. This has significant implications to ion-implantation processes used for both applied and fundamental experimental purposes, since most implantation is done at room temperature and much that has previously been reported has neglected any discussion of the flux dependence of the process. In addition, we have determined that the critical dependence of flux on temperature has an activation energy of  $E_a = 0.9 \pm 0.05$  eV, as opposed to the higher  $E_a = 1.2 \pm 0.05$  eV determined at

higher temperatures for noble gas irradiation of Si.<sup>4,5</sup> This is attributed to a fundamentally different mechanism for the amorphization, involving the dynamic collapse of complex defect structures via point-defect emission.

We are grateful to Richard Goldberg for his assistance with the RBSC measurements at RMIT. One of us (P.J.S.) would like to acknowledge partial support for this research from the Natural Sciences and Engineering Research Council of Canada, and support from the Electronic Materials Engineering Department at ANU.

\*Permanent address: Department of Physics, University of Western Ontario, London, Ontario, N6A 3K7, Canada.

†Microelectronics and Materials Technology Centre, Royal Melbourne Institute of Technology, Melbourne 3000, Australia.

<sup>1</sup>J. F. Gibbons, Proc. IEEE **60**, 1062 (1972).

<sup>2</sup>J. W. Corbett, J. P. Karins, and T. Y. Tan, Nucl. Instrum. Methods **182/183**, 457 (1981).

<sup>3</sup>F. L. Vook and H. J. Stein, Radiat. Eff. **2**, 23 (1969).

<sup>4</sup>R. G. Elliman, J. Linnros, and W. L. Brown, Mater. Res. Soc. Symp. Proc. **100**, 363 (1988).

<sup>5</sup>J. Linnros, R. G. Elliman, and W. L. Brown, J. Mater. Res. **3**, 1208 (1988).

<sup>6</sup>G. D. Watkins and J. W. Corbett, Phys. Rev. **138**, 543 (1965).

<sup>7</sup>L. J. Cheng, J. C. Corelli, J. W. Corbett, and G. D. Watkins, Phys. Rev. **152**, 761 (1966).

<sup>8</sup>J. H. Freeman, D. J. Chivers, G. A. Gard, G. W. Hinder, B. J. Smith, and J. Stephen, in *Ion Implantation in Semiconductors*, edited by S. Namba (Plenum, New York, 1975), p. 555.

<sup>9</sup>We found variations of 50%–100% in the damage produced when samples were simply mechanically clamped to the copper mounting block, without using a coupling grease.

<sup>10</sup>G. D. Watkins, J. Phys. Soc. Jpn. **18**, Suppl. II, 22 (1963).

<sup>11</sup>J. Bourgoin and M. Lannoo, *Point Defects in Semiconductors II: Experimental Aspects* (Springer-Verlag, Berlin, 1983), Chap. 9.

<sup>12</sup>J. A. Davies, J. Denhartog, L. Eriksson, and J. W. Mayer, Can. J. Phys. **45**, 4053 (1967).

<sup>13</sup>T. Y. Tan, in *Defects in Semiconductors*, edited by J. Narayan and T. Y. Tan, MRS Symposia Proceedings No. 2 (North Holland, New York, 1981), p. 163.

<sup>14</sup>Simple planar multivacancies are illustrated in Ref. 2.